An assessment of a simplified methodology for determining the thermal performance of thermo-active piles

Author 1 (corresponding author)

- Ryan Yin Wai Liu, MEng, ACGI, PhD, DIC, AFHEA
- Department of Civil and Environmental Engineering, Imperial College London, London, United Kingdom
- ORCID number: 0000-0002-5278-6426
- Room 430, Skempton Building, Imperial College London, London, SW7 2AZ
- ryl13@ic.ac.uk

Author 2

- David M.G. Taborda, MEng, PhD, DIC
- Department of Civil and Environmental Engineering, Imperial College London, London, United Kingdom
- ORCID number: 0000-0001-5391-2087

ABSTRACT

Ground source energy systems provide low-carbon heating and cooling to buildings, but their efficient deployment requires a reliable estimate of their thermal performance. A simplified methodology is presented to determine the thermal performance of thermo-active piles when heating or cooling loads are specified with either inlet pipe temperatures or imposed heat fluxes. The proposed methodology avoids computationally expensive 3D analyses and the explicit simulation of heat exchanger pipes, relying instead on 2D thermal analyses. When the heating or cooling of a thermo-active pile is assessed by imposing inlet pipe temperatures, the proposed methodology allows the determination of the power of pile per unit length. Conversely, when heating or cooling loads are specified via extracted or injected heat fluxes, the inlet and outlet fluid temperatures, as well as average temperatures at pile wall, are determined. The proposed methodology has been shown to reproduce accurately the thermal performance of thermo-active piles modelled using 3D analyses where heat exchanger pipes are explicitly simulated, considering different patterns of heating and cooling cycles. The application of the proposed methodology to the case of a real thermo-active pile is demonstrated by comparing its predicted thermal performance with the results of a well-documented field thermal response test.

LIST OF NOTATIONS

A	Area
D	Pile diameter
F_0	Fourier number
k	Thermal conductivity
k_{soil}	Thermal conductivity of the ground
L	Pile length
$n_{U-loops}$	Number of U-loops within the thermo-active pile
P	Power of pile per unit length

Q	Flow rate of carrier fluid
Q_{total}	Total flow rate of carrier fluid
r	Radial distance
r_{pile}	Pile radius
r_{pipes}	The radial distance measured from the pile centre at which the pipes are located within the thermo-active pile
T_{av}	Average temperature of carrier fluid
T_{in}	Inlet fluid temperature
$T_{initial}$	Initial ground temperature
$T_{in,av}$	Average inlet fluid temperature
$T_{in,mid}$	Temperature of fluid in the pipe going down the pile at pile mid-depth
T_{out}	Outlet fluid temperature
$T_{out,av}$	Average outlet fluid temperature
$T_{out,mid}$	Temperature of fluid in the pipe going up the pile at pile mid-depth
T_{tbc}	The temperature that is prescribed as a thermal boundary condition in the axisymmetric analysis
t	Time
α_{soil}	Thermal diffusivity of the ground
ΔE	Assumed power per unit length of the thermo-active pile
ΔH	Change in energy content per unit length
ΔT_{wall}	Average change in temperature at pile wall
ρC_p	Volumetric heat capacity

Φ_g G-function

1. INTRODUCTION

In order to reduce carbon emissions and fulfil sustainability targets, there is a need to explore technologies which do not rely on fossil fuels to provide heating and cooling, such as thermo-active piles (Amis & Loveridge, 2014; Sani et al., 2019; Loveridge et al., 2022). Compared with conventional piles, this type of foundations combines the role of providing structural stability with that of exchanging heat with the ground, supplying low carbon heating and cooling when coupled with a heat pump. Local sustainability targets, such as the Merton Rule, which requires a proportion of the energy demand of a building to be generated on site using renewable sources (Merton Council, 2010; World Wide Fund For Nature, 2019), play an important role in promoting the use of thermo-active piles, as designing geotechnical structures to work as heat exchangers is particularly advantageous in dense urban environments where space for other renewable energy sources is scarce. As a result, it is vitally important to correctly estimate the thermal performance of thermo-active piles, and hence the savings in energy spent on heating or cooling when such foundations are incorporated into the design of a building to ensure that the building's energy demand can be met and the relevant regulations are complied with.

The thermal performance of thermo-active piles is commonly quantified in terms of power (i.e. energy extracted/injected from/into the ground per unit time) per unit pile length. However, the power that can be delivered by thermo-active piles is not a quantity that is easy to determine as it is dependent on many factors, such as the difference between inlet temperature (i.e. the temperature of fluid entering the thermo-active pile) and the ground temperature (Nagano et al., 2005; Gao et al., 2008; You et al., 2014), operation mode (i.e. whether the thermo-active piles are operated continuously or intermittently) (You et al., 2014; Faizal et al., 2016; Li et al., 2021a; Li et al., 2021b), number of heat exchanger pipe U-loops within the thermo-active piles (Hamada et al., 2007; Gao et al., 2008; Brettman et al., 2010; Jalaluddin et al., 2011) and flow rate of carrier fluid (Gao et al., 2008; Jalaluddin et al., 2011; You et al., 2014; Park et al., 2017). Although Brandl (2006) suggested it can generally be assumed that thermo-active piles with diameters $0.3 - 0.5\ m$ can achieve thermal performances of $40 - 60\ W \cdot m^{-1}$, and piles with diameters $\geq 0.6\ m$ can achieve $35\ W$ per m^2 of earth-contact area, a review (Liu, 2022) on the thermal performance of thermo-active piles has shown that the power of thermo-active piles can vary from lower than $20\ W \cdot m^{-1}$ (e.g. Henderson et al. (1998)) to higher than $250\ W \cdot m^{-1}$ (e.g. Sekine et al. (2007)).

To estimate the thermal performance of a thermo-active pile, the two most commonly used methods are G-functions (Loveridge & Powrie, 2013; Pagola et al., 2018) and three-dimensional (3D) thermal numerical analyses (Gao et al., 2008; Batini et al., 2015; Cecinato & Loveridge, 2015; Liu et al., 2020a). The former have been successfully adapted from techniques used to design borehole heat exchangers, and are typically limited in their ability to provide information about the power per unit pile length, as they are mainly focused on solving temperature changes given an applied heat flux. On the other hand, 3D thermal numerical analyses, which include the explicit simulation of heat exchanger pipes, can be conducted, as performed by Gao et al. (2008), Batini et al. (2015), Cecinato and Loveridge (2015) and Liu et al. (2020a). However, these 3D analyses are computationally expensive and the explicit simulation of heat exchanger pipes, where heat transfer is dominated by advection, presents considerable computational challenges. Therefore, a simplified method that does not involve 3D analyses or simulation of heat exchanger pipes to predict the thermal performance of thermo-active piles is proposed in this paper, with its accuracy being assessed by comparing with 3D numerical analyses with the explicit simulation of heat exchanger pipes using COMSOL Multiphysics (COMSOL AB, 2022). Moreover, as highlighted by Bourne-Webb et al. (2020), the heating/cooling of a thermo-active pile is commonly modelled using either a prescribed temperature (e.g. Salciarini et al., 2017; Vieira & Maranha, 2017; Rammal et al., 2018; Liu et al., 2020b) or a heat flux thermal boundary condition (e.g. Di Donna & Laloui, 2015; Alberdi-Pagola et al., 2017; Liu et al., 2019; Sani & Singh, 2020). Therefore, the simplified methodology proposed herein considers these two alternative modelling approaches. Section 2 details the methodology to estimate the power per unit pile length of a thermo-active pile when given a prescribed temperature thermal boundary condition, while Section 3 details the methodology to estimate the inlet and outlet fluid temperatures, as well as the average pile wall temperature, when a prescribed heat flux is given. The simplified methodology is then applied in Section 4 to the prediction of the thermal performance of a thermo-active pile for which the results of a field thermal response test are available (Loveridge et al., 2014). Note that throughout this paper, the convention is that positive power refers to heat injection into the ground (i.e. cooling of the building) and vice versa for negative values.

2. AN APPROACH BASED ON FLUID TEMPERATURE

2.1 The methodology

When the inlet fluid temperature is specified for the heating or cooling of a thermo-active pile, the most accurate way to model the thermal performance of the thermo-active pile is, as mentioned above, to conduct a 3D analysis where the heat exchanger pipes are explicitly modelled. The temperature specified is then prescribed as the inlet temperature of the carrier fluid, and the power of the thermo-active pile per unit length P $[W \cdot m^{-1}]$ can be calculated from the volumetric heat capacity of the carrier fluid ρC_p $[J \cdot m^{-3} \cdot K^{-1}]$, flow rate of the fluid Q $[m^3 \cdot s^{-1}]$, pile length L $[m]$, and the temperature differential between the heat exchanger pipe inlet(s) and outlet(s) $T_{in} - T_{out}$ $[K]$ according to Equation (1), where $n_{U-loops}$ is the number of U-loops within the thermo-active pile.

$$P = \sum_{i}^{n_{U-loops}} \frac{\rho C_p \cdot Q_i}{L} \cdot (T_{in} - T_{out})_i \tag{1}$$

The proposed approach is based on the fundamental idea that the heat exchange phenomena taking place in the thermo-active pile can be adequately captured by conducting a 2D thermal analysis where the heating or cooling from the heat exchanger pipes is modelled by a temperature thermal boundary condition prescribed at where the heat exchanger pipes are realistically located within the thermo-active pile cross-section. The power evolution of the thermo-active pile can then be deduced from the average change in temperature of the system (i.e. due to conservation of energy). A 2D thermal analysis is expected to be a reasonable approach as piles tend to be relatively slender (i.e. one dimension considerably larger than the others), therefore, a section of the pile at mid-length approximates 2D conditions.

Step 1 – Determine the thermal boundary condition for the 2D thermal analysis

In the 2D thermal analysis, a constant temperature boundary condition is applied to the nodes belonging to the inner circumferences of the heat exchanger pipes. The temperatures that are prescribed, $T_{in,mid}$ $[K]$ for the case of a heat exchanger pipe where the fluid circulates downwards and $T_{out,mid}$ $[K]$ for heat exchanger pipes where the fluid circulates upwards, are determined from the inlet temperature T_{in} $[K]$ and outlet temperature T_{out} $[K]$ of each U-loop.

By assuming a linear variation of temperature along the heat exchanger pipes, $T_{in,mid}$ and $T_{out,mid}$ can be determined using Equations (2) and (3), respectively.

$$T_{in,mid} = T_{in} - (T_{in} - T_{out}) \times \frac{1}{4} \quad (2)$$

$$T_{out,mid} = T_{in} - (T_{in} - T_{out}) \times \frac{3}{4} \quad (3)$$

In this context, T_{in} is the specified temperature for the heating/cooling of the thermo-active pile, while T_{out} can be evaluated using Equation (4), which is based on conservation of energy and was employed by Liu et al. (2020b). In Equation (4), ΔE $[W \cdot m^{-1}]$ is the assumed power injected (positive ΔE) or extracted (negative ΔE) from the thermo-active pile per unit pile length. Note that this quantity differs from P, as P is the exact true power that is injected or extracted from the thermo-active pile, whereas ΔE is just an assumed power that is solely used to estimate T_{out}. Liu et al. (2020b) have shown that a ΔE based on 35 W per m^2 of earth-contact area, which follows the recommendation by Brandl (2006) for piles with diameters $\geq$ 600 mm, provides a relatively accurate estimation of the temperature field within and around the thermo-active pile, and hence the resulting thermal-mechanical pile response. However, this is based only on heating the thermo-active pile with an inlet temperature of 20℃ above the initial ground temperature. As it is expected that the thermal performance of a thermo-active pile increases with the difference between the inlet temperature and the initial ground temperature (Nagano et al., 2005; Gao et al., 2008; You et al., 2014), the expression for ΔE is normalised in this paper according to Equation (5), where D $[m]$ is the pile diameter and $T_{initial}$ $[K]$ is the initial ground temperature. The need for this approach will be justified later in the paper when a T_{in} that varies with time is considered.

$$T_{out} = T_{in} - \frac{\Delta E \cdot L}{n_{U-loops} \cdot \rho C_p \cdot Q} \quad (4)$$

$$\Delta E = 35\ [W/m^2] \cdot \pi D \cdot \frac{T_{in} - T_{initial}}{20\ [K]} \quad (5)$$

Step 2 – Conduct the 2D thermal analysis

By adopting the temperature thermal boundary conditions $T_{in,mid}$ and $T_{out,mid}$ determined from Step 1 at the inner circumferences of the heat exchanger pipes, a 2D transient thermal analysis is conducted to simulate the evolution of the temperature field of the entire system, which consists of the thermo-active pile cross-section and the soil surrounding it, over the entire duration where the thermal performance of the thermo-active pile has to be evaluated. Note that the domain boundary must be sufficiently far from the pile edge to avoid boundary effects.

Step 3 – Determine the change in energy content of the thermo-active pile and soil

Due to conservation of energy, the power of the thermo-active pile per unit length P is equal to the change in energy content of the entire system (i.e. pile and soil) per unit length ΔH $[J \cdot m^{-1}]$ per unit time t $[s]$, according to Equation (6).

$$P = \frac{\Delta(\Delta H)}{\Delta t} \tag{6}$$

The change in energy content of the entire system is equal to the sum of changes in energy content over each section (i.e. pile and soil) within the system, according to Equation (7), while the change in energy content of each section can be evaluated by integrating the change in temperature $(T - T_{initial})$ $[K]$ of the section over its area A $[m^2]$, multiplied by its volumetric heat capacity ρC_p $[J \cdot m^{-3} \cdot K^{-1}]$, according to Equation (8).

$$\Delta H = \sum_i \Delta H_i \tag{7}$$

$$\Delta H_i = \rho C_{p,i} \cdot \int_{A_i} (T_i - T_{initial})\, dA_i \tag{8}$$

2.2 Demonstration of the method

The accuracy of the proposed simplified method to estimate the thermal performance of a thermo-active pile is assessed using three different inlet temperature signals:

- Constant inlet temperature (Section 2.2.1)
- Inlet temperature that varies sinusoidally with a period of one year, correspondingly roughly to a heating season and a cooling season per year (Section 2.2.2)

- Inlet temperature that varies sinusoidally with a period of a month superimposed to one that varies sinusoidally with a period of one year, in order to simulate higher frequency events (Section 2.2.3)

In all of the above cases, a thermo-active pile with 900 mm diameter and 20 m length with double U-loop (also known as 2U) pipe arrangement is considered. The adopted mesh and domain, as well as the layout of the heat exchanger pipes within the thermo-active pile cross-section, where the inner pipe diameter is 26.2 mm with a concrete cover of 70 mm, are illustrated in Figure 1(a) and (b). The carrier fluid is assumed to be water with a flow rate of $1 \times 10^{-4}\ m^3/s$ per U-loop and volumetric heat capacity of $4.18 \times 10^6\ J \cdot m^{-3} \cdot K^{-1}$. The thermo-active pile is located at the centre of a 80 m by 80 m domain, and its boundaries are prescribed with a thermal boundary condition where the temperature is not allowed to vary from its initial value. The initial temperature of the system is 20℃ and the thermal properties of the thermo-active pile and the surrounding soil are given in Table 1. All analyses are conducted using COMSOL.

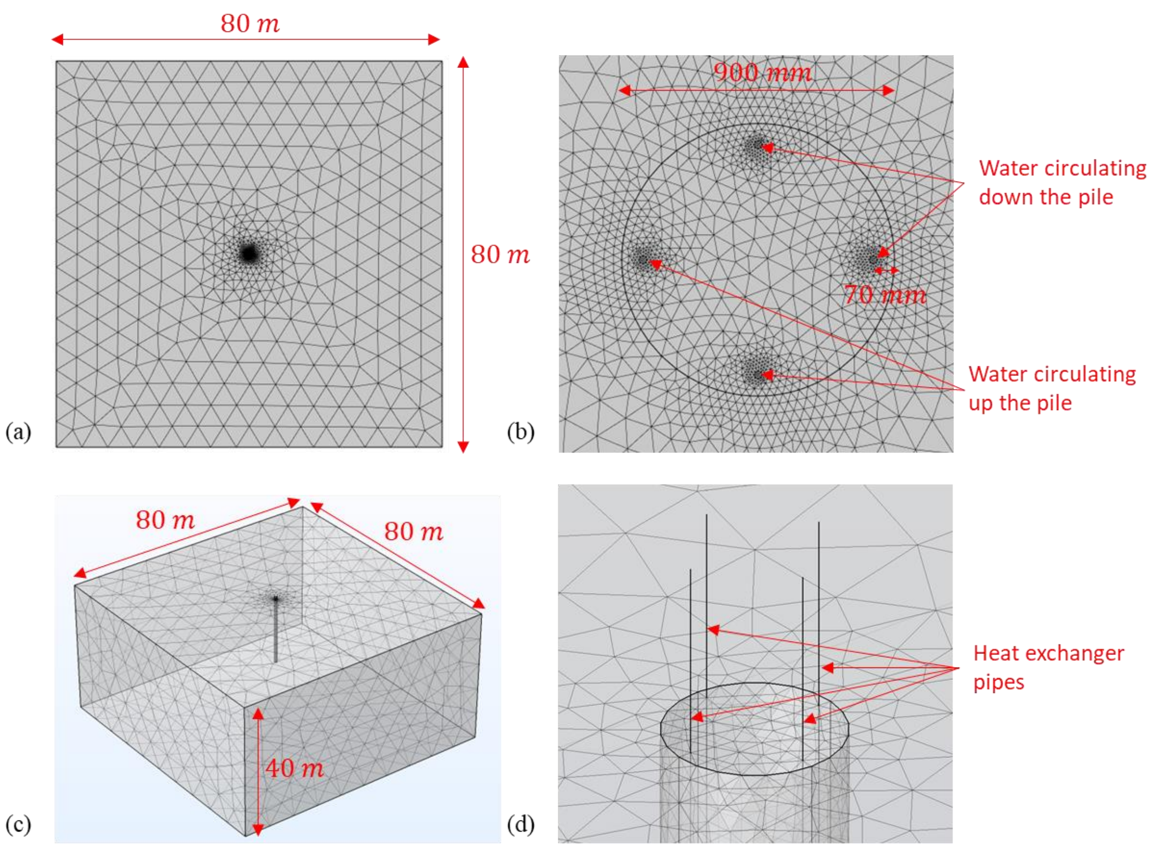

Figure 1 (a) Mesh and domain adopted in the 2D analysis; (b) detail of the thermo-active pile and layout of heat exchanger pipes in the 2D analysis; (c) mesh and domain adopted in the 3D analysis; (d) detail of the thermo-active pile and heat exchanger pipes in the 3D analysis

Table 1 Thermal properties of the thermo-active pile concrete and soil

	Concrete	Soil
Thermal conductivity k $[W \cdot m^{-1} \cdot K^{-1}]$	2.3	1.8
Volumetric heat capacity ρC_p $[J \cdot m^{-3} \cdot K^{-1}]$	1.9×10^6	1.8×10^6

In order to assess the accuracy of the simplified method, the obtained results are compared against those from benchmark 3D analyses where heat exchanger pipes are explicitly simulated. The mesh and domain that are adopted in these benchmark analyses are illustrated in Figure 1(c) and (d). Note that these analyses are also conducted using COMSOL, where the dimensions of the domain are $80\,m \times 80\,m \times 40\,m$, and the heat exchanger pipes are simulated using one-dimensional elements specifically formulated for this purpose. All domain boundaries are prescribed a thermal boundary condition where the temperature is not allowed to vary from its initial value. The heat exchanger pipe walls are modelled with a thickness of 2.9 mm and have a thermal conductivity of 0.4 $W \cdot m^{-1}$ (Loveridge et al., 2014; Gawecka et al., 2020).

2.2.1 Constant inlet temperature

A constant inlet temperature of $T_{in} = 40$°C, which is 20°C above the initial ground temperature, is considered. Note that the value of temperature chosen is merely illustrative and it does not affect the validity of the method, which can be used for any mode of operation (i.e. heating or cooling). According to Equations (2) to (5), this would result in $\Delta E = 99\ W \cdot m^{-1}$, $T_{out} =$ 37.6°C, $T_{in,mid} = 39.4$°C and $T_{out,mid} = 38.2$°C. The thermal boundary conditions of $T_{in,mid}$ and $T_{out,mid}$ are then prescribed at the inner circumferences of the heat exchanger pipes within the thermo-active pile cross-section, as illustrated in Figure 2. The 2D thermal analysis is run for one year and the evolution of power of the thermo-active pile per unit length obtained from Equations (6) to (8) is shown in Figure 3. Also shown in Figure 3 is the power obtained from the benchmark 3D analysis where heat exchanger pipes are explicitly simulated, calculated according to Equation (1).

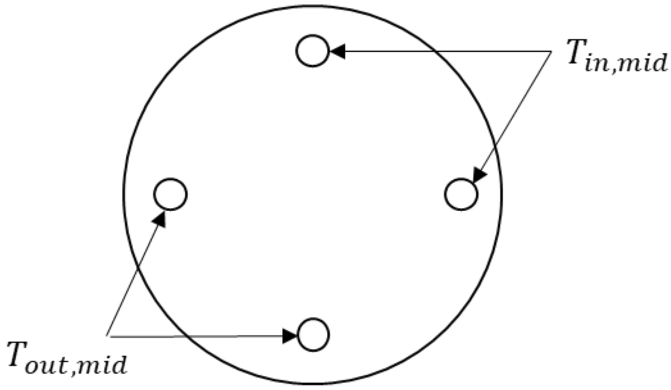

Figure 2 Illustration of the thermal boundary condition for the 2D thermal analysis

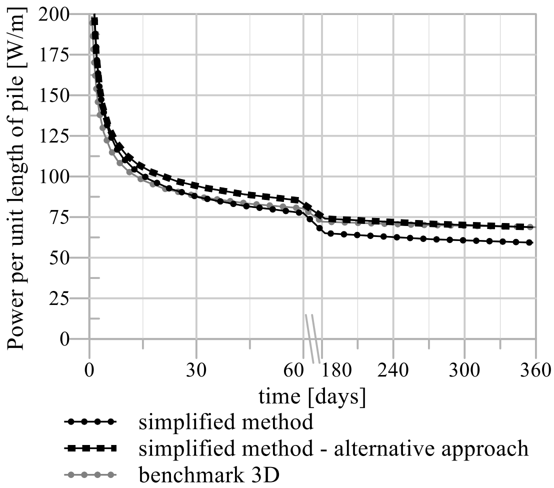

Figure 3 Evolution of power per unit pile length with time for the case of constant inlet temperature

It can be observed from Figure 3 that the power of the thermo-active pile is initially high due to the steep thermal gradient between the hot heat exchanger pipe and cold thermo-active pile. As time progresses, the thermo-active pile and soil are heated up and the thermal gradient is reduced, hence the power reduces significantly and reaches a relatively constant value after 360 days of operation. It can also be observed that the proposed simplified method is capable of predicting the power of the thermo-active pile accurately up to around 60 days of operation. After this point, the simplified method tends to underestimate slightly the power and, after 360 days of operation, the power is underestimated by 14%. Clearly, this is due to the assumption of an infinitely long thermo-active pile, which is inherent to a 2D analysis. The power of an infinitely long thermo-active pile is smaller than that from a pile with finite length, due to the absence of vertical thermal flux (i.e. in the direction of the pile axis) in the former case. In effect, the modelling of a 2D section of a thermo-active pile necessarily implies that heat flux is solely radial. Conversely, when a 3D analysis is performed, the presence of the ground surface and a soil deposit below the tip of the thermo-active pile leads to vertical heat flux taking place, in addition to the aforementioned radial heat flux, which enhances heat transfer from the thermo-active pile to the ground. Moreover, the constant temperature boundary condition adopted at the surface allows heat losses from the soil surrounding the thermo-active pile to take place, further contributing to maintaining a higher thermal gradient between the heat exchanger pipes, thermo-active pile and the soil. Naturally, this effect only manifests itself after long periods of sustained operation, allowing heat to propagate from the heat exchanger pipes to the surface boundary through the soil.

Although it has been shown that the proposed simplified method is sufficiently accurate in predicting short-term thermal performance, when long-term thermal performance is the subject of consideration, an alternative approach, which is similar to the one adopted by Liu et al. (2020b), can be adopted. In this alternative approach, following the 2D thermal analysis, an average temperature along the circumference with $r = r_{pipes}$ (where r is a radial coordinate measured from the centre of the thermo-active pile and r_{pipes} is the radial distance between the centre of thermo-active pile and the centre of heat exchanger pipes) is calculated for each time-step, generating a time-dependent temperature T_{tbc}. After this, an axisymmetric thermal analysis is conducted where the heating/cooling of the thermo-active pile is modelled by prescribing T_{tbc} within the pile at $r = r_{pipes}$. A simple approach to measure the energy loss through the surface boundary (where a boundary condition specifying no change in temperature is again adopted) is to include a very thin layer of material with a very high volumetric heat capacity (e.g. 1000 times that of soil) above it. This layer can absorb a large amount of energy without any significant change in temperature, while the surface of this material is modelled as adiabatic. The energy loss through the soil surface can then be approximated by the change in energy content of this layer. The power of the thermo-active pile can hence be determined by conservation of energy, in a manner similar to that described in Step 3 above. Alternatively, the energy losses through the top boundary could be calculated by integrating over the surface area the heat flux normal to this boundary.

The thermal performance obtained using the alternative approach outlined above (where an axisymmetric thermal analysis is conducted following a 2D thermal analysis) is compared with those from the benchmark 3D analysis and the original simplified method in Figure 3. It can be observed that, in addition to the short-term thermal performance, where the error is limited to about 8%, the long-term thermal performance has been successfully captured with high degree of accuracy using this alternative approach.

2.2.2 Inlet temperature that varies sinusoidally with a period of one year

A simplified simulation of a typical year with one heating season and one cooling season is carried out using a sinusoidal inlet temperature described by the function $T_{in}(t) = 20 + 20 \cdot \sin\left(\frac{2\pi t}{360}\right)$. This inlet temperature corresponds to an amplitude of 20°C with a period of one year varying around the initial ground temperature of 20°C, meaning that the fluid temperature oscillates between 0°C and 40°C. As a result, $\Delta E, T_{out}, T_{in,mid}$ and $T_{out,mid}$ are all functions of time. Similar to Section 2.2.1, the thermal boundary conditions of $T_{in,mid}$ and $T_{out,mid}$ are prescribed at the inner circumferences of the heat exchanger pipes within the thermo-active pile cross-section and the 2D thermal analysis is run for one year. The computed evolution with time of power per unit pile length is shown on Figure 4, together with the power obtained from the benchmark 3D analysis. It can be observed from Figure 4 that the simplified method provides a very accurate estimation of the thermal performance throughout one year of operation, where the maximum power during pile heating has only been underestimated by 0.8%, while during pile cooling the maximum power has only been overestimated by 2.7%.

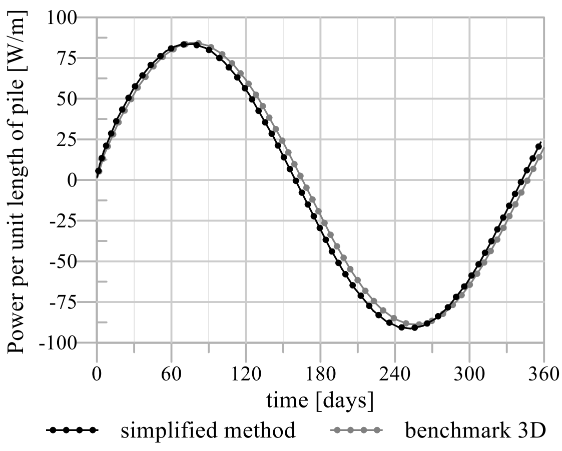

Figure 4 Evolution of power per unit pile length with time for the case of sinusoidal inlet temperature

2.2.3 Inlet temperature that varies sinusoidally with a period of one year plus monthly cycles

This is a case which builds upon the one considered in Section 2.2.2, with monthly cycles with amplitude of 10°C being added to the inlet temperature signal, for which the expression is now given by: $T_{in} = 20 + 20 \cdot \sin\left(\frac{2\pi t}{360}\right) + 10 \cdot \sin\left(\frac{2\pi t}{30}\right)$. The 2D thermal analysis is run for one year and the evolution of power per unit pile length with time is compared in Figure 5 to power obtained from the corresponding benchmark 3D analysis. Clearly, Figure 5 demonstrates that the simplified method provides a very accurate estimation of the thermal performance, with the various peaks in power delivered by the thermo-active pile being generally overestimated by less than 15%, an error that reduces to a maximum of 10% when only the largest peaks are considered (around 60 days for heating and 250 days for cooling). It is also interesting to note that, as the frequency of temperature oscillations increases, the accuracy of the proposed methodology appears to improve substantially. This is perhaps unsurprising: high frequency temperature variations tend to mostly affect the concrete in the immediate vicinity of the heat exchanger pipes, thus reducing the influence of the heat losses through the soil surface, which is clearly the main contributor to the observed differences between the 3D analysis and the proposed methodology based on 2D thermal analyses. Moreover, it should be appreciated that in all the three cases considered above (Sections 2.2.1 to 2.2.3), the temperatures within the soil are accurately reproduced by the simplified method. Further discussions on temperature predictions by the simplified method will be presented in Section 3.

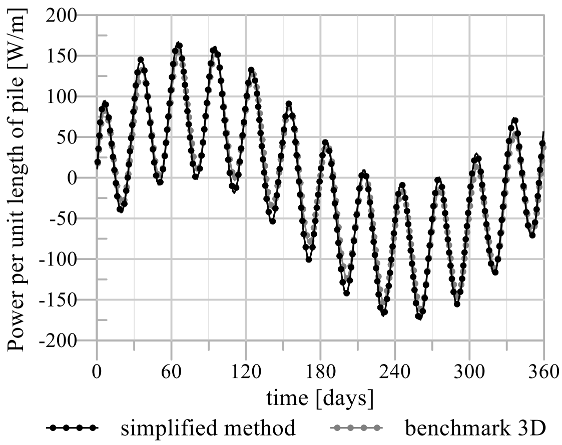

Figure 5 Evolution of power per unit pile length with time for the case of sinusoidal inlet temperature plus monthly cycles

3. AN APPROACH BASED ON TRANSFERRED HEAT

3.1 The methodology

When the heating or cooling of a thermo-active pile is modelled by specifying a heat flux per unit pile length P $[W \cdot m^{-1}]$, the most accurate way to determine the inlet and outlet fluid temperatures (which are dependent on the amount of energy transferred to/from the thermo-active pile), as well as the average temperature at the pile wall, is to conduct a 3D analysis where the heat exchanger pipes are explicitly modelled. In order to estimate the above quantities without the use of 3D analyses and the simulation of heat exchanger pipes, a methodology based on 2D thermal analysis, such as the one described in Section 2.1, is proposed.

In the proposed approach, a 2D transient thermal analysis is conducted with the heating or cooling from the heat exchanger pipes being modelled by applying the heat flux P $[W \cdot m^{-1}]$ uniformly over the areas defined by the inner diameter of the pipes. This ensures that the heat sources are realistically located within the thermo-active pile cross-section. The analysis is conducted to simulate the evolution of the temperature field of the entire system, which consists of the thermo-active pile cross-section and the soil surrounding it. Following the analysis, the evolution with time of the average temperature of the carrier fluid T_{av} $[K]$ is estimated by that of the elements representing the heat exchanger pipes in the thermo-active pile cross-section (to which the thermal properties of the carrier fluid have been assigned). Assuming that this average fluid temperature is given by $T_{av} = \frac{1}{2}\left(T_{in,av} + T_{out,av}\right)$, the average inlet temperatures $T_{in,av}$ $[K]$ and outlet temperatures $T_{out,av}$ $[K]$ (note that the term 'average' is used as they represent the average of the inlet or outlet temperatures when more than one U-loops of heat exchanger pipes are used) can be estimated using Equations (9) and (10). As expected, in Equations (9) and (10), a total carrier fluid flow rate Q_{total} $[m^3 \cdot s^{-1}]$ is required to estimate the temperature distributions.

$$T_{in,av} = T_{av} + \frac{P \cdot L}{2 \cdot \rho C_p \cdot Q_{total}} \tag{9}$$

$$T_{out,av} = T_{av} - \frac{P \cdot L}{2 \cdot \rho C_p \cdot Q_{total}} \tag{10}$$

3.2 Demonstration of the method

The accuracy of the proposed simplified method when estimating operating fluid temperatures and average temperature changes at pile wall is assessed using two different heat flux signals:

- Constant heat flux (Section 3.2.1)
- Heat flux that varies sinusoidally with a period of one year, approximating a typical year which includes a heating season and a cooling season (Section 3.2.2)

In both of the cases above, the thermo-active pile modelled is identical to the one considered in Section 2.2 (see Figure 1(a) and (b) for further details of the numerical model), where the carrier fluid is assumed to be water, with a volumetric heat capacity of $4.18 \times 10^6\, J \cdot m^{-3} \cdot K^{-1}$ and thermal conductivity of $0.6\, W \cdot m^{-1} \cdot K^{-1}$, while the thermal properties of thermo-active pile and soil follow those given in Table 1.

Benchmark 3D analyses where heat exchanger pipes are explicitly modelled are conducted in order to allow the accuracy of the simplified method to be assessed. These benchmark 3D analyses are similar to those described in Section 2.2 (see Figure 1(c) and (d)), with the exception of the boundary condition used to simulate heating or cooling: as proposed in Sailer (2020), rather than prescribing an inlet temperature at the pipe inlets, the pipe inlets are now connected to the pipe outlets to form closed circuits, with the specified heat flux bring prescribed to the fluid before it is recirculated back into the ground, as illustrated in Figure 6.

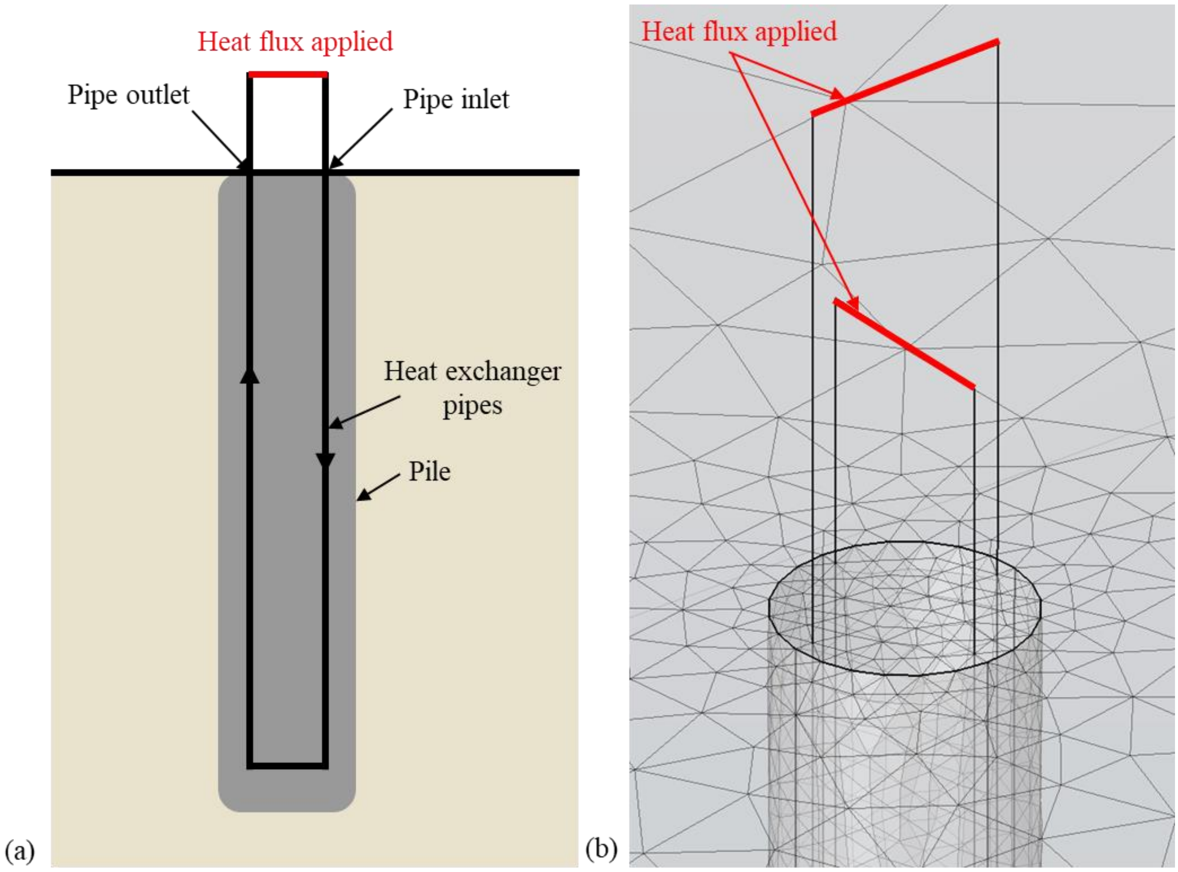

Figure 6 Application of heat flux in the benchmark 3D analyses: (a) illustration of the approach and (b) implications to the numerical model.

3.2.1 Constant heat flux

A constant heat flux of 100 $W \cdot m^{-1}$, which corresponds to a total heat flux of 2000 W is considered. According to the simplified method, a heat flux of 100 W is prescribed uniformly over the heat exchanger pipe cross-sections, and for a 2U pipe arrangement with four heat exchanger pipes in the thermo-active pile cross-section, each pipe shares a heat flux of 25 W.

The 2D thermal analysis is run for one year and the evolution of average fluid temperature T_{av} with time is shown in Figure 7, together with the average fluid temperature ($T_{av} = \frac{1}{2}(T_{in,av} + T_{out,av})$) obtained in the benchmark 3D analysis, while Figure 8 compares the inlet and outlet temperatures derived from the 2D thermal analysis using Equations (9) and (10) with the average inlet and outlet temperatures obtained from the benchmark 3D analysis.

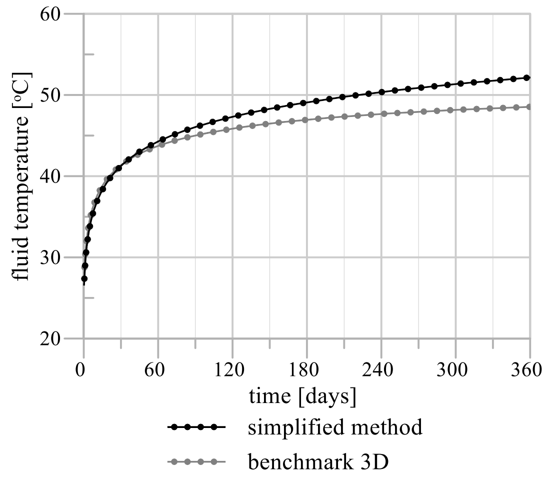

Figure 7 Evolution of average fluid temperature with time for the case of constant heat flux

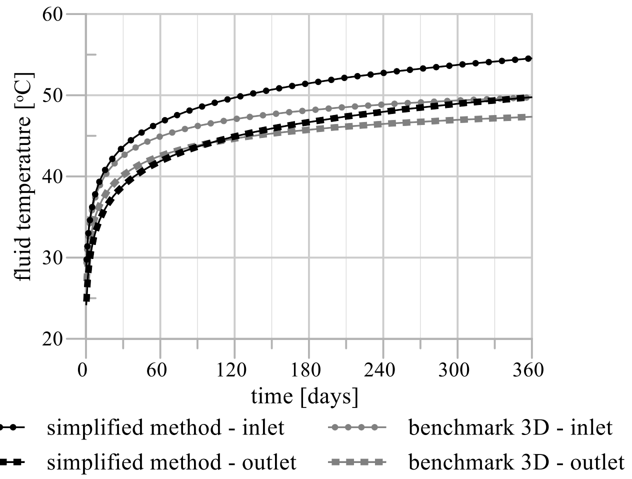

Figure 8 Evolution of inlet and outlet temperatures with time for the case of constant heat flux

Referring to Figure 7 and Figure 8, it can be observed that the fluid temperatures increase rapidly during the initial stages of the analyses, with the heating rate slowing down with time. This suggests that, when the fluid is initially cold, the thermal gradient between the fluid and the thermo-active pile is small and little heat transfer takes place from the fluid into the thermo-active pile; therefore, most of the energy from the applied heat flux is stored within the fluid and hence its temperature increases rapidly. With time, as the fluid temperature increases, significant heat transfer takes place from the fluid into the thermo-active pile; therefore, a smaller proportion of energy from the applied heat flux is stored within the fluid and hence the increase in temperature slows down considerably.

It is also interesting to note that both the average fluid temperature (Figure 7) and the estimated inlet and outlet temperatures (Figure 8) are captured accurately by the simplified method up to around 60 days of operation. After this stage, as had been observed in Section 2.2, the simplified method consistently overestimates the fluid temperatures (i.e. underestimates the performance of the thermo-active pile). However, after one year of operation, the differences in terms of change in inlet and outlet temperatures are limited to about 15% and 10%, respectively. As seen previously, this overestimation is due to the 2D simplification of the problem, as the 2D analysis is unable to capture the effects of the ground surface, which in the benchmark 3D analysis is modelled as a surface with no change in temperature that dissipates energy from the system. Therefore, more energy accumulates within the system in the 2D analysis which explains the higher fluid temperatures observed when sufficient time has elapsed.

Figure 9 compares the evolution of average pile wall temperature change with time modelled between the simplified method and the benchmark 3D analysis. Note that, in Figure 9, the evolutions of average pile wall temperature change with time are presented as G-functions (same as those presented in Loveridge and Powrie (2013)), where the average pile wall temperature change ΔT_{wall} $[K]$ is normalised as Φ_g according to Equation (11), and time t $[s]$ is normalised as the Fourier number F_0 according to Equation (12). In Equations (11) and (12), k_{soil} $[W \cdot m^{-1} \cdot K^{-1}]$ is the thermal conductivity of the ground, P $[W \cdot m^{-1}]$ is the applied heat flux per unit pile length, α_{soil} $[m^2 \cdot s^{-1}]$ is the thermal diffusivity of the ground and r_{pile} $[m]$ is the radius of the thermo-active pile.

Figure 9 further confirms that the simplified method produces similar patterns in terms of average temperature change as those obtained in the benchmark 3D analysis until the contribution of boundary effects manifests itself. Also shown in Figure 9 are the upper and lower bounds G-functions proposed by Loveridge and Powrie (2013) for thermo-active piles with an aspect ratio (AR) of 25 (which is close to the AR of 22.2 for the thermo-active pile considered in this study). It can be observed that the G-function from the benchmark 3D analysis lies within the range defined by the upper and lower bounds, and so does that from simplified method before the onset of boundary effects.

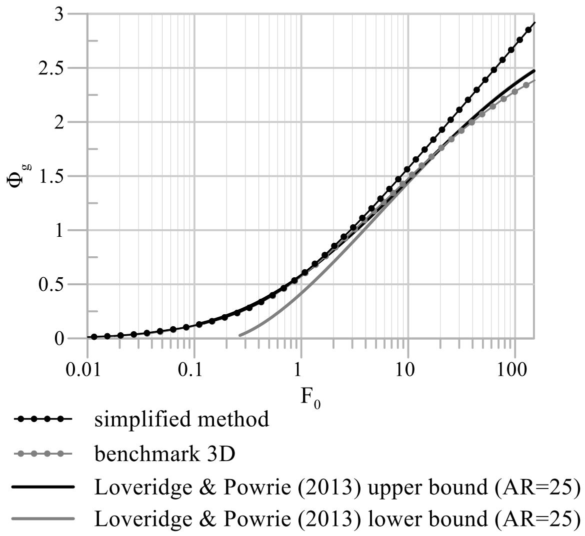

Figure 9 G-functions for the case of constant heat flux

$$\Phi_g = \frac{2\pi k_{soil}}{P} \Delta T_{wall} \tag{11}$$

$$F_0 = \frac{\alpha_{soil} t}{r_{pile}^2} \tag{12}$$

3.2.2 Heat flux that varies sinusoidally with a period of one year

A final test of the proposed methodology consists of applying a heat flux per unit length of $P = 100 \cdot \sin\left(\frac{2\pi t}{360}\right)\ [W \cdot m^{-1}]$, which corresponds to a signal amplitude of $100\ W \cdot m^{-1}$ with a period of one year. Similar to the case considered in Section 3.2.1, the heat flux is prescribed uniformly over the heat exchanger pipe cross-sections (i.e. each pipe shares a heat flux of $25 \cdot \sin\left(\frac{2\pi t}{360}\right)\ W$) in the simplified method. The 2D thermal analysis is run for one year and the inlet and outlet temperatures derived (using Equations (9) and (10)) are compared in Figure 10 with the average inlet and outlet temperatures from the benchmark 3D analysis. It can be observed from Figure 10 that the simplified methodology provides an accurate estimation of the inlet and outlet fluid temperatures throughout the entire period of operation, where the maximum error in terms of the peak change in inlet or outlet fluid temperatures is less than 8%. Such high precision further reinforces the conclusion drawn from the results of the analyses where an inlet temperature is applied: the accuracy of the simplified method is considerably higher for boundary conditions which are more transient in nature, such as those expected to dominate operational patterns of real heat pumps.

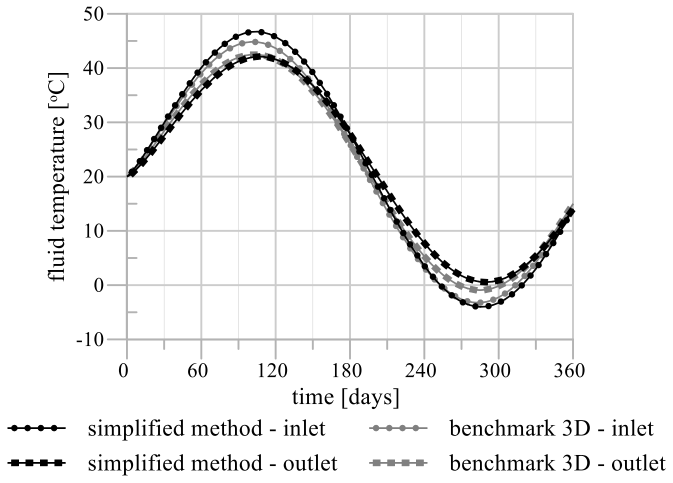

Figure 10 Evolution of inlet and outlet temperatures with time for the case of sinusoidal variation of heat flux with a period of one year

4. APPLICATION TO A CASE STUDY

In order to demonstrate the practical application of the proposed simplified methodology for estimating the thermal performance of real thermo-active piles, the field thermal response test (TRT) conducted by Loveridge et al. (2014) is considered. In this field TRT, the thermo-active pile has a diameter of 300 mm over the top 26.8 m and 200 mm below that, extending to an unreported depth. A single U-loop pipe arrangement is adopted where the heat exchanger pipes are installed to a depth of 26 m and have a concrete cover of 82.5 mm. The internal pipe diameter is 26.2 mm with a pipe wall thickness of 2.9 mm. The pile is founded in London Clay and water is used as the carrier fluid with a flow rate of $1.032 \times 10^{-4}\ m^3 \cdot s^{-1}$. The thermal properties of the thermo-active pile, soil and water used to simulate this field TRT are listed in Table 2 (Loveridge et al., 2014; Gawecka et al., 2020). Note that the initial ground temperature is 17.7℃.

Table 2 Thermal properties of the thermo-active pile concrete, soil and water used to simulate the field TRT (Loveridge et al., 2014; Gawecka et al., 2020)

	Concrete	Soil	Water
Thermal conductivity $k\ [W \cdot m^{-1} \cdot K^{-1}]$	2.0	2.4	0.6

Volumetric heat capacity ρC_p $[J \cdot m^{-3} \cdot K^{-1}]$	1.8×10^6	2.15×10^6	4.18×10^6

The time histories of both the actual power applied and mean fluid temperatures are provided in Loveridge et al. (2014), allowing the validation of both approaches outlined by the simplified methodology: estimation of power per metre of pile based on known fluid temperatures (Section 2) and estimation of fluid temperatures based on applied power (Section 3). Note that only the first 7.5 days of the field test are considered for brevity, which include 4.5 days of circulating water at ambient temperature, followed by 3 days of pile heating (i.e. simulating cooling mode).

4.1 Estimation of power based on fluid temperatures

The mean fluid temperature (which equates to the average of inlet and outlet temperatures) provided in Loveridge et al. (2014) is converted into inlet temperatures (see Gawecka et al. (2020) for further details regarding the conversion), the time history of which is presented in Figure 11. This allows the application of the simplified methodology outlined in Section 2.

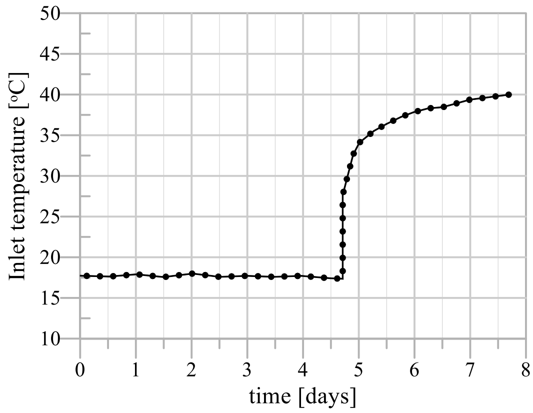

Figure 11 Applied evolution of inlet temperature with time

The simplified methodology is applied as outlined in Section 2.1, leading to the evolution of power per unit pile length shown in Figure 12. Compared to the power applied in the field ($\sim 86\ W \cdot m^{-1}$), which is reported in Loveridge et al. (2014) but not used in the present calculations, it can be seen that the proposed approach results in an overestimation of the thermal performance of the thermo-active pile limited to 15% ($\sim 100\ W \cdot m^{-1}$). Clearly, given the level of approximations involved in the proposed methodology, this level of accuracy is very satisfactory. However, this estimate can be further refined by using the estimated thermal performance as the “assumed power”, ΔE, in Equation (4), rather than using Equation (5), leading to a short iterative procedure: the new estimated thermal performance, shown in Figure 13 as “iteration 2” is now ~90 $W \cdot m^{-1}$, i.e. within ~5% of the value observed in the field. To demonstrate the rapid convergence of this procedure, a new iteration is performed by adopting this value as ΔE leading to the results illustrated in Figure 13 (“iteration 3”). These are clearly indistinguishable from the previous iteration, meaning that further simulations are not required.

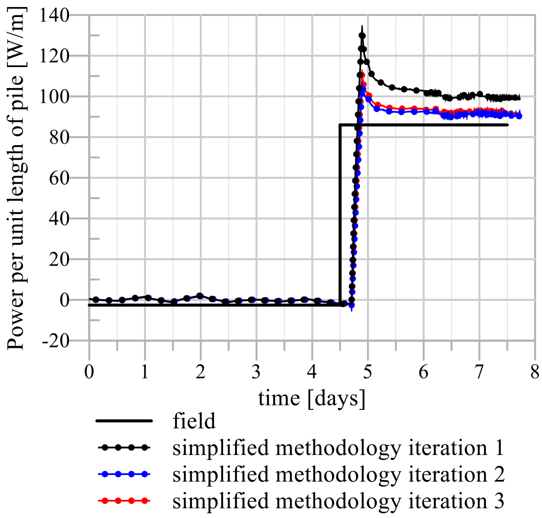

Figure 12 Power per unit pile length estimated by the simplified methodology compared against those applied in the field

4.2 Estimation of fluid temperatures based on applied power

In order to estimate the mean fluid temperatures based on the applied power in the field test (measured as $-2.58\, W \cdot m^{-1}$ for 4.5 days, followed by $85.96\, W \cdot m^{-1}$ for 3 days), the procedure outlined in Section 3.1 is employed. The time evolution of the mean fluid temperature estimated by the simplified methodology is compared with the measured values from the field in Figure 13. As can be seen, the simplified methodology has resulted in an overestimation of the mean fluid temperature limited to ~7.6%. Considering all the approximations involved (no simulation of vertical heat flux, potential heterogeneity of the thermal properties of the soil, etc.) the small value obtained for the calculated error once again demonstrates the excellent accuracy of the simplified methodology.

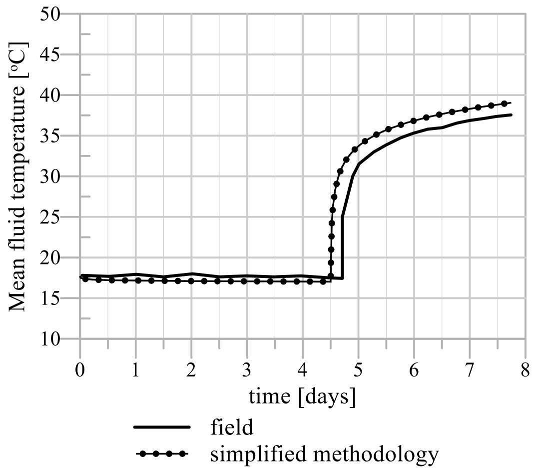

Figure 13 Time evolution of mean fluid temperature estimated by the simplified methodology compared against those measured in the field

5. CONCLUSIONS

This paper puts forward a simplified methodology to estimate the thermal performance of a thermo-active pile. The proposed methodology involves only 2D analyses and therefore avoids the use of computationally expensive 3D analyses as well as the explicit simulation of heat exchanger pipes. Since the operation of a thermo-active pile is usually modelled using either a prescribed temperature approach or a prescribed heat flux approach, the methodology is detailed for both cases, with 3D analyses where heat exchanger pipes are explicitly simulated being used as benchmark.

When the heating or cooling of a thermo-active pile is simulated based on an inlet pipe temperature, the proposed methodology seeks to determine the power of the pile per unit length. This is accomplished by performing a 2D thermal analysis, where a given temperature is prescribed at the heat exchanger pipes, allowing the power of the thermo-active pile to be determined from the change in energy content of the system. Three different patterns of operation were considered – constant inlet temperature, sinusoidal variation of inlet temperature with a period of one year and sinusoidal variation of inlet temperature with a period of one month – with the proposed methodology showing good agreement with the benchmark 3D analyses. For the case where a constant inlet temperature is applied, the proposed method was seen to be conservative, underestimating the thermal performance by 14% after one year of operation. This is due to heat losses through the surface, which cannot be captured in 2D thermal analyses. However, it should be noted that the accuracy of the adopted modelling approach increased substantially with the increase in frequency of the variation of inlet temperature, for the case where a sinusoidal variation of inlet temperature with a period of one year is applied, the error of the proposed method is reduced to $1-3\%$. This improved performance is clearly associated with the reduced importance of the ground surface for highly transient variations in fluid temperature.

In the second part of this paper, the heating or cooling of a thermo-active pile is specified by a heat flux, with the proposed methodology seeking to determine the inlet and outlet fluid temperatures as well as the average temperature at the pile wall. This is again accomplished by performing a 2D thermal analysis, where heat flux thermal boundary conditions are prescribed at the heat exchanger pipes (the thermal properties of which are modelled to be the same as the carrier fluid), and the inlet and outlet fluid temperatures can be inferred from the average temperature of the elements representing the heat exchanger pipes. Similar performance is observed as in the case of specified inlet temperature: the proposed methodology is seen to be conservative, underpredicting slightly the thermal performance, with carrier fluid temperatures being overestimated by about $10-15\%$ after one year of operation. However, when a higher frequency sinusoidal variation of the flux is used, which is closer to more realistic operational patterns of ground source energy systems, the accuracy increases significantly, with the maximum error in terms of peak change in inlet or outlet fluid temperatures reduces to less than 8%.

In the final part of the paper, the practical capability of the simplified methodology is validated through the consideration of a field thermal response test where the time histories of both mean fluid temperature and applied power are well-documented. Both approaches of the simplified methodology: estimation of power from given fluid temperatures and estimation of fluid temperatures from given applied power, have been shown to yield accurate estimates of the observed field performance of the thermo-active pile. The power and mean fluid temperature estimated by the simplified methodology exhibit only a small error ($\sim 5\%$ and $\sim 8\%$, respectively) compared to the field values. This result underscores the excellent accuracy of the simplified methodology.

ACKNOWLEDGEMENTS

This research is part of the SaFEGround (Sustainable, Flexible and Efficient Ground-source heating and cooling systems) project, which is funded by the Engineering and Physical Sciences Research Council (EPSRC) (grant number: EP/V042149/1). For the purpose of open access, the authors have applied a Creative Commons Attribution (CC BY) licence to any Author Accepted Manuscript version arising.

REFERENCES

Alberdi-Pagola, M., Madsen, S., Jensen, R. & Poulsen, S. (2017) Numerical Investigation on the Thermo-Mechanical Behavior of a Quadratic Cross Section Pile Heat Exchanger. In: *Proceedings of the IGSHPA Technical/Research Conference and Expo 2017,*

Amis, A. & Loveridge, F. (2014) Energy Piles and Other Thermal Foundations for Gshp–Developments in Uk Practice and Research. *Rehva journal*, **2014** (1), 32-35.

Batini, N., Rotta Loria, A. F., Conti, P., Testi, D., Grassi, W. & Laloui, L. (2015) Energy and Geotechnical Behaviour of Energy Piles for Different Design Solutions. *Applied Thermal Engineering*, **86**, 199-213.

Bourne-Webb, P., Zito, M., Bodas Freitas, T. M. & Sterpi, D. (2020) Effect of Thermal Boundary Conditions on the Response of Thermally-Activated Floating Piles in a Cohesive Material. *E3S Web of Conferences*, **195**.

Brandl, H. (2006) Energy Foundations and Other Thermo-Active Ground Structures. *Geotechnique*, **56** (2), 81-122.

Brettman, T., Amis, T. & Kapps, M. (2010) Thermal Conductivity Analysis of Geothermal Energy Piles. *Proceedings of the 2010 Geotechnical Challenges in Urban Regeneration Conference, London, UK*. pp. 26-28.

Cecinato, F. & Loveridge, F. A. (2015) Influences on the Thermal Efficiency of Energy Piles. *Energy*, **82**, 1021-1033.

COMSOL AB (2022) Comsol Multiphysics Version 6.0, www.comsol.com. COMSOL AB, Stockholm, Sweden.

Di Donna, A. & Laloui, L. (2015) Numerical Analysis of the Geotechnical Behaviour of Energy Piles. *International Journal for Numerical and Analytical Methods in Geomechanics*, **39** (8), 861-888.

Faizal, M., Bouazza, A. & Singh, R. M. (2016) An Experimental Investigation of the Influence of Intermittent and Continuous Operating Modes on the Thermal Behaviour of a Full

Scale Geothermal Energy Pile. *Geomechanics for Energy and the Environment*, **8**, 8-29.

Gao, J., Zhang, X., Liu, J., Li, K. & Yang, J. (2008) Numerical and Experimental Assessment of Thermal Performance of Vertical Energy Piles: An Application. *Applied Energy,* **85** (10), 901-910.

Gawecka, K. A., Taborda, D. M. G., Potts, D. M., Sailer, E., Cui, W. & Zdravković, L. (2020) Finite-Element Modeling of Heat Transfer in Ground Source Energy Systems with Heat Exchanger Pipes. *International Journal of Geomechanics*, **20** (5).

Hamada, Y., Saitoh, H., Nakamura, M., Kubota, H. & Ochifuji, K. (2007) Field Performance of an Energy Pile System for Space Heating. *Energy and Buildings*, **39** (5), 517-524.

Henderson, H., Carlson, S. & Walburger, A. (1998) North American Monitoring of a Hotel with Room Size G.S.H.P.S. *Proceedings of the IEA 1998 Room Size Heat Pump Conference*.

Jalaluddin, Miyara, A., Tsubaki, K., Inoue, S. & Yoshida, K. (2011) Experimental Study of Several Types of Ground Heat Exchanger Using a Steel Pile Foundation. *Renewable Energy*, **36** (2), 764-771.

Li, R., Kong, G., Chen, Y. & Yang, Q. (2021a) Thermomechanical Behaviour of an Energy Pile–Raft Foundation under Intermittent Cooling Operation. *Geomechanics for Energy and the Environment*, **28**.

Li, R., Kong, G., Sun, G., Zhou, Y. & Yang, Q. (2021b) Thermomechanical Characteristics of an Energy Pile-Raft Foundation under Heating Operations. *Renewable Energy*, **175**, 580-592.

Liu, R. Y. W., Taborda, D. M. G., Gawecka, K. A., Cui, W. & Potts, D. M. (2019) Computational Study on the Effects of Boundary Conditions on the Modelled Thermally Induced Axial Stresses in Thermo-Active Piles. *Proceedings of the XVII European Conference on Soil Mechanics and Geotechnical Engineering, Reykjavik, Iceland*.

Liu, R. Y. W., Sailer, E., Taborda, D. M. G. & Potts, D. M. (2020a) Evaluating the Impact of Different Pipe Arrangements on the Thermal Performance of Thermo-Active Piles. *E3S Web of Conferences*, **205**.

Liu, R. Y. W., Sailer, E., Taborda, D. M. G., Potts, D. M. & Zdravković, L. (2020b) A Practical Method for Calculating Thermally-Induced Stresses in Pile Foundations Used as Heat Exchangers. *Computers and Geotechnics*, **126**.

Liu, R. Y. W. (2022) *Numerical Modelling of Complex Thermo-Hydro-Mechanical Interactions in Thermo-Active Pile Foundations*. PhD thesis. Imperial College London, London.

Loveridge, F. & Powrie, W. (2013) Temperature Response Functions (G-Functions) for Single Pile Heat Exchangers. *Energy*, **57**, 554-564.

Loveridge, F., Powrie, W. & Nicholson, D. (2014) Comparison of Two Different Models for Pile Thermal Response Test Interpretation. *Acta Geotechnica*, **9** (3), 367-384.

Loveridge, F., Schellart, A., Rees, S., Stirling, R., Taborda, D., Tait, S., Alibardi, L., Biscontin, G., Shepley, P., Shafagh, I., Shepherd, W., Yildiz, A. & Jefferson, B. (2022) Heat Recovery and Thermal Energy Storage Potential Using Buried Infrastructure in the Uk. *Proceedings of the Institution of Civil Engineers - Smart Infrastructure and Construction*, **175** (1), 10-26.

Merton Council (2010) *Sustainable Design and Construction Evidence Base: Climate Change in the Planning System*. Merton Council.

Nagano, K., Katsura, T., Takeda, S., Saeki, E., Nakamura, Y., Okamoto, A. & Narita, S. (2005) Thermal Characteristics of Steel Foundation Piles as Ground Heat Exchangers. *Proceedings of the 8th International Energy Agency Heat Pump Conference 2005, Las Vegas, USA*.

Pagola, M. A., Jensen, R. L., Madsen, S. & Poulsen, S. E. (2018) *Method to Obtain G-Functions for Multiple Precast Quadratic Pile Heat Exchangers*. Aalborg University. DCE Technical Reports, No. 243.

Park, S., Lee, D., Lee, S., Chauchois, A. & Choi, H. (2017) Experimental and Numerical Analysis on Thermal Performance of Large-Diameter Cast-in-Place Energy Pile Constructed in Soft Ground. *Energy*, **118**, 297-311.

Rammal, D., Mroueh, H. & Burlon, S. (2018) Impact of Thermal Solicitations on the Design of Energy Piles. *Renewable and Sustainable Energy Reviews*, **92**, 111-120.

Sailer, E. (2020) *Numerical Modelling of Thermo-Active Retaining Walls*. PhD Thesis. Imperial College London, London.

Salciarini, D., Ronchi, F. & Tamagnini, C. (2017) Thermo-Hydro-Mechanical Response of a Large Piled Raft Equipped with Energy Piles: A Parametric Study. *Acta Geotechnica*, **12** (4), 703-728.

Sani, A. K., Singh, R. M., Amis, T. & Cavarretta, I. (2019) A Review on the Performance of Geothermal Energy Pile Foundation, Its Design Process and Applications. *Renewable and Sustainable Energy Reviews*, **106**, 54-78.

Sani, A. K. & Singh, R. M. (2020) Response of Unsaturated Soils to Heating of Geothermal Energy Pile. *Renewable Energy*, **147**, 2618-2632.

Sekine, K., Ooka, R., Yokoi, M., Shiba, Y. & Hwang, S. (2007) Development of a Ground-Source Heat Pump System with Ground Heat Exchanger Utilizing the Cast-in-Place Concrete Pile Foundations of Buildings. *Ashrae Transactions*, **113** (1).

Vieira, A. & Maranha, J. R. (2017) Thermoplastic Analysis of a Thermoactive Pile in a Normally Consolidated Clay. *International Journal of Geomechanics*, **17** (1), 04016030.

World Wide Fund For Nature (2019) Climate Mitigation by Merton Rule, Available from: https://wwf.panda.org/?204444/Merton-London-climate-rule [Accessed: 20th February 2020]

You, S., Cheng, X., Guo, H. & Yao, Z. (2014) In-Situ Experimental Study of Heat Exchange Capacity of C.F.G. Pile Geothermal Exchangers. *Energy and Buildings*, **79**, 23-31.